Research Square

Preprints are preliminary reports that have not undergone peer review.
They should not be considered conclusive, used to inform clinical practice,
or referenced by the media as validated information.

Bayesian Small Area Estimation of District-Level Malaria Prevalence in Nigeria Using the 2021 Malaria Indicator Survey

Olamide Akeboi
Corona Management Systems
Maris Raymond
maris.raymond@coronams.com

Corona Management Systems
David Bassey
Corona Management Systems
Abba Christian
Corona Management Systems
Debra Okeh
Corona Management Systems
Obi Charles
Corona Management Systems
Adaeze Eche-George
Corona Management Systems
Ganiyat Eshikhena
Corona Management Systems
Chukwu Okoronkwo
National Malaria Elimination Programme
Eze Nelson
National Malaria Elimination Programme
Ezra Gayawan
Federal University of Technology
Nnenna Chizaram Ogbulafor
National Malaria Elimination Programme
Godwin Ntadom
Federal Ministry of Health
Chijioke Kaduru
Corona Management Systems

Article

Keywords: Malaria, Small area estimation, Bayesian hierarchical model, Nigeria, Local Government Area, Spatial epidemiology, Rapid diagnostic test, Microscopy

Posted Date: November 16th, 2026

DOI: https://doi.org/10.21203/rs.3.rs-11391144/v1

License: This work is licensed under a Creative Commons Attribution 4.0 International License.
Read Full License

Additional Declarations: No competing interests reported.

Title

Bayesian Small Area Estimation of District-Level Malaria Prevalence in Nigeria Using the 2021 Malaria Indicator Survey

Authors

Olamide Akeboi[1,2,4], Maris Raymond[1,2*], David Bassey[1,2], Abba Christian[2], Debra Okeh[1,2], Obi Charles[1,2], Adaeze Eche-George[2], Ganiyat Eshikhena[1,2], Chukwu Okoronkwo[3], Eze Nelson[3], Ezra Gayawan[4], Nnenna Chizaram Ogbulafor[3], Godwin Ntadom[5], Chijioke Kaduru[1,2]

Affiliations

1. African Institute of Modelling and Analytics, Nigeria
2. Corona Management Systems, Kado-Abuja, Nigeria
3. National Malaria Elimination Programme, Abuja, Nigeria
4. Department of Statistics, Federal University of Technology, Akure, Nigeria
5. Department of Public Health, Federal Ministry of Health, Abuja, Nigeria

*** Corresponding author:** maris.raymond@coronams.com

Other author emails: olamide.akeboi@coronams.com, david.bassey@coronams.com, abba.christian@coronams.com, debra.okeh@coronams.com, obi.charles@coronams.com, adaeze.echegeorge@coronams.com, eshikhena@coronams.com, chukoro_christ@yahoo.co.uk, ezenelson24@gmail.com, egayawan@futa.edu.ng, nnennanco@yahoo.com, ntadomg@yahoo.com, kaduru@coronams.com

Abstract

Background

The Nigeria Malaria Indicator Survey (NMIS) provides robust national and state-level estimates but cannot support reliable estimates at the district or Local Government Area (LGA) level, the resolution the National Malaria Elimination Programme (NMEP) uses for intervention planning. In this study, we applied Bayesian small area estimation to the 2021 NMIS to estimate prevalence for all 774 LGAs, providing a platform for similar analysis for future NMIS.

Methods

Using rapid diagnostic test (RDT) and microscopy outcomes from the 2021 NMIS, geospatial covariates and routine health management information system records (HMIS), we fitted a Bayesian hierarchical spatial model via integrated nested Laplace approximation. We assessed robustness using stochastic partial differential equation (SPDE), hierarchical pooling, and joint RDT–microscopy alternative models with shared spatial fields.

Results

Of the774 LGAs, 352 contained no surveyed cluster and relied entirely on spatial smoothing and covariates. Estimates reproduced the established northwest-to-southeast transmission gradient, driven principally by household wealth and global P falciparum prevalence. Applying NMEP's operational thresholds yielded sharply different tier assignments: RDT classified 48.6% of LGAs as high transmission versus 10.6% by microscopy. A joint diagnostic model revealed that RDT and microscopy share a common national spatial pattern but diverge credibly in nine states.

Conclusions

These LGA-level estimates broadly reflect Nigeria's established malaria transmission gradient and support NMEP planning. However, transmission classification may vary by diagnostic method, suggesting the need to standardise diagnostics or review tier thresholds. Applying this approach to smaller planning units and future NMIS could strengthen malaria programme planning.

Keywords

Malaria; Small area estimation; Bayesian hierarchical model; Nigeria; Local Government Area; Spatial epidemiology; Rapid diagnostic test; Microscopy

1. Introduction

Accurate subnational estimates of disease burden are increasingly vital for effective public health planning and equitable resource distribution in low- and middle-income countries (LMICs) [1]. However, there is a pronounced disconnect between national survey aggregates and the granular data required for subnational decision-making [2]. National averages frequently mask significant spatial disparities across smaller geographic units, hiding local inequalities in disease prevalence and healthcare access [1].

In Nigeria, this disconnect poses a critical challenge for controlling malaria, which remains a leading cause of morbidity and mortality. Nigeria continues to bear the highest malaria burden worldwide [3]. Malaria transmission in the country is characterised by profound spatial heterogeneity, driven by diverse ecological zones ranging from mangrove swamps and rainforests in the south to Sahel savannahs in the north [4, 5]. These varied environments, combined with socioeconomic disparities and varying vector distributions, drastically influence local transmission intensity across different administrative units and local government areas [6].

To track this burden, Malaria surveillance in Nigeria relies heavily on nationally representative surveys such as the Malaria Indicator Survey (MIS) and Demographic and Health Survey (DHS), which provide essential data on malaria prevalence, intervention coverage, and risk factors for national and state-level planning. While these surveys have been instrumental in monitoring trends and informing policy [4, 7], their sampling design does not support reliable estimates at finer geographic levels, such as Local Government Areas (LGAs), creating a critical gap for targeted malaria interventions [8]. This limitation creates a critical disconnect between the granularity of data required for targeted public health interventions and the resolution of data available from traditional survey mechanisms.

Small Area Estimation (SAE) provides a critical statistical framework to bridge these data sparsity gaps. SAE techniques, particularly Bayesian hierarchical modelling (BHM), synthesise sparse survey data with auxiliary geospatial covariates to "borrow strength" across related areas [1]. By integrating spatial correlation and quantifying uncertainty, Bayesian SAE generates stable, high-resolution prevalence maps that reveal hidden hotspots of disease transmission [1, 9, 10]. The application of Integrated Nested Laplace Approximations (INLA) within these models facilitates fast Bayesian inference, making it computationally feasible to process large datasets and generate timely estimates for numerous wards across Nigeria's vast landscape This approach is essential for Nigeria's National Malaria Elimination Programme, which requires granular data to optimise the allocation of limited resources, target chemoprevention, R2I and insecticide-treated net distributions, and monitor progress toward elimination goals in high-burden LGAs [6, 9].

Several studies have attempted to map malaria risk in Nigeria, but critical gaps remain, particularly regarding the spatial resolution of the estimates. For instance, previous research applying Bayesian geostatistical modelling produced continuous spatial risk maps on a pixel grid rather than actionable estimates aggregated at the administrative LGA level [4]. Similarly, studies exploring spatial inequalities have conducted their analyses at the broader state level, which fails to capture deep localised disparities within those states [11]. While some studies

have estimated malaria metrics across all 774 LGAs, such as the work by Ozodiegwu et al. [6], the study utilised agent-based mathematical modelling that grouped districts into broader epidemiological archetypes to simulate intervention scenarios, rather than estimating empirical prevalence directly for each district. Other studies have focused exclusively on highly localised urban contexts, such as mapping childhood malaria hotspots in specific cities [12]. Furthermore, while advanced Bayesian geospatial modelling has been successfully utilised to map high-resolution malaria risk in other sub-Saharan African countries like Ghana [8], there remains a notable scarcity of research adapting these advanced Bayesian SAE techniques to provide comprehensive, nationwide district-level prevalence estimates in Nigeria. Therefore, the aim of this study is to estimate district-level malaria prevalence in Nigeria using Bayesian small area estimation of the 2021 Malaria Indicator Survey.

To address this gap, this study was developed in collaboration with NMEP, which identified the need for microscopy-based LGA-level prevalence estimates to support the 2026–2030 National Malaria Strategic Plan. We extended the analysis to include RDT to examine whether diagnostic choice materially affects transmission-tier classification. NMEP subsequently endorsed this expanded scope, recognising its implications for resource-allocation guidance. Accordingly, this study aims to estimate LGA-level malaria prevalence in Nigeria using Bayesian small area estimation of the 2021 Malaria Indicator Survey, comparing microscopy- and RDT-based estimates.

2. Methods

2.1 Study Setting

Estimation targets Nigeria's 774 Local Government Areas (LGAs), the country's third-tier administrative division and the resolution at which the National Malaria Elimination Programme (NMEP) plans and allocates malaria-control interventions. LGA boundaries were obtained from GRID3 Nigeria and used both for choropleth mapping and, via queen contiguity, to construct the spatial adjacency structure described in Section 2.3.

2.2 Data sources

The data sources and covariates included in the analysis are summarised below, highlighting the variables obtained from each source and how they were derived and incorporated into the analysis.

Data source	Covariates/variables derived	Data processing/model use
2021 Nigeria Malaria Indicator Survey (NMIS)	Malaria prevalence from RDT and microscopy; household wealth score; proportion of households classified as urban; cluster GPS coordinates	RDT and microscopy results from children aged 6–59 months were used as outcome data. Household wealth and urban/rural status were calculated as survey-weighted LGA-level means. GPS coordinates were used to assign survey clusters to LGAs.

Malaria Atlas Project (MAP)	*P. falciparum* parasite rate; *P. falciparum* prevalence; *P. falciparum* incidence; ITN use; IRS coverage; *P. falciparum* mortality	Extracted at LGA level using the malariaAtlas R package.
DHS Geospatial Covariates	Enhanced vegetation index; aridity; elevation; population density	Cluster-level values were averaged across survey clusters within each LGA.
WorldClim 2021	Precipitation; maximum temperature; minimum temperature	Climate surfaces were extracted at LGA level.
GRID3	Health-facility density	Health-facility locations were spatially joined to LGA boundaries and expressed per 1,000 children aged 1–4 years using WorldPop population estimates.
WorldPop	Under-five population counts	Used as the population denominator for calculating health-facility density.
Routine Health Management Information System (HMIS)	Test-positivity rate; HMIS-calibrated prevalence	Test-positivity rates were calibrated against survey-based prevalence before inclusion in the analysis.

2.3 Model Specification

LGA-level prevalence was estimated using a Bayesian hierarchical spatial model of the Besag–York–Mollié family (BYM [13]) in its reparameterised BYM2 form [15]. RDT and microscopy outcomes were modelled independently, given documented differences in the sensitivity and specificity of the two diagnostics [14]. The data model, including the latent process and parameter model, is described below.

Data model. For LGA $i = 1, \ldots, 774$, let Y_i denote the number of children under five testing positive out of N_i tested. The number of positive tests was modelled as binomial:

$$Y_i \mid p_i \sim \text{Binomial}(N_i, p_i) \quad \text{logit}(p_i) = \eta_i$$

$$\eta_i = \beta_0 + \Sigma_k \beta_k x_{ik} + b_i$$

where x_{ik} are the k standardised covariates in the selected candidate set (Section 2.6) and b_i is the spatial random effect defined below.

Latent process. The BYM2 spatial term [15] combines a spatially structured and an unstructured component in a single, interpretable convolution:

$$b_i = (1/\sqrt{\tau_b}) \cdot \left(\sqrt{\frac{\varphi}{s}} u_i \; + \; \sqrt{1-\varphi} v_i \right)$$

where $u \sim \mathrm{ICAR}(W)$ is an intrinsic Gaussian Markov random field on the LGA adjacency graph W; $v_i \sim N(0,1)$ independently; τ_b is the marginal precision of b; $\varphi \in [0,1]$ is the proportion of variance attributable to the spatially structured component; and s is a graph-dependent scaling constant [16] so that φ is interpretable independently of the specific adjacency structure used.

Parameter model. τ_b was assigned a penalised-complexity (PC) prior [17] with $P(\sigma_b > 1) = 0.01$, and φ a PC prior with $P(\varphi < 0.5) = 0.5$, following the defaults recommended by Riebler et al. [15]. Fixed effects were assigned diffuse Gaussian priors, $N(0,\ 0.001)$. A sum-to-zero constraint was imposed on the spatial random effect for identifiability, and the Sørbye and Rue [16] scaling was applied.

2.4 Model Implementation

Models were fitted by integrated nested Laplace approximation (INLA [18]) in R-INLA, using the adaptive Gaussian approximation strategy with empirical Bayes integration over hyperparameters (INLA's eb strategy). Analyses used the R packages spdep for adjacency construction, sf for spatial data handling, srvyr for design-based estimation, and malariaAtlas for raster covariate extraction.

2.5 Transmission-intensity Classification

Following the classification scheme of Nigeria's National Malaria Elimination Programme (NMEP), LGAs were categorised into High (≥35%), Moderate A (15-<35%), Moderate B (10-<15%), Low A (5-<10%), Low B (1-<5%) and Very low (<1%) transmission settings using NMEP's operational malaria prevalence thresholds (1%, 5%, 10%, 15%, and 35%) which were applied to each LGA's posterior mean prevalence [19]. The World Health Organization classifies malaria transmission intensity into four main categories: high, moderate, low, and very low transmission settings using indicative thresholds for *P. falciparum* prevalence among children aged 2–10 years ($PfPR_{2–10}$) and incidence rates. High-transmission settings are characterised by a $PfPR_{2–10}$ of approximately ≥35%. Moderate transmission corresponds to a $PfPR_{2–10}$ of approximately 10–35%. Low-transmission settings are characterised by a $PfPR_{2–10}$ of approximately 1–10%. Very low transmission is generally characterised by a $PfPR_{2–10}$ of <1%, with areas approaching elimination having progressively lower levels of parasite prevalence. [20]

2.6 Model comparison and diagnostics

Eight candidate covariate sets per diagnostic (Table 1) were compared using the Watanabe–Akaike information criterion (WAIC [21]) and the deviance information criterion (DIC [22]). The lowest-WAIC set for both diagnostics combined a ten-covariate baseline (parasite rate, vegetation index, aridity, elevation, household wealth, health-facility density, population density, proportion urban, precipitation, and maximum temperature) with global P. falciparum parasite rate and incidence surfaces and was used for the final model reported in Section 3.

125 ***Table 1. Covariates considered and their composition across the eight candidate sets1***

Covariate	B	+G	+H	+Hc	+Ap	+Af	+HA	+M
Baseline covariates								
MAP P. falciparum parasite rate	✓	✓	✓	✓	✓	✓	✓	✓
Enhanced vegetation index	✓	✓	✓	✓	✓	✓	✓	✓
Aridity index	✓	✓	✓	✓	✓	✓	✓	✓
Elevation	✓	✓	✓	✓	✓	✓	✓	✓
Household wealth index	✓	✓	✓	✓	✓	✓	✓	✓
Health-facility density (per 1,000 under-five)	✓	✓	✓	✓	✓	✓	✓	✓
Population density	✓	✓	✓	✓	✓	✓	✓	✓
Proportion urban	✓	✓	✓	✓	✓	✓	✓	✓
Precipitation, 2021	✓	✓	✓	✓	✓	✓	✓	✓
Maximum temperature, 2021	✓	✓	✓	✓	✓	✓	✓	✓
MAP global disease-surface additions								
MAP P. falciparum prevalence surface		✓						
MAP malaria incidence surface		✓						
Routine health-system additions								
HMIS test-positivity rate			✓				✓	
HMIS-calibrated prevalence				✓				
DHS geospatial archetype additions								
Archetype P. falciparum prevalence					✓	✓	✓	
Archetype ITN use, under-five						✓	✓	
Archetype under-five treatment coverage						✓	✓	
MAP intervention-raster additions								
ITN use raster								✓
IRS coverage raster								✓

	P. falciparum mortality raster	✓

B = baseline; +G = baseline + MAP global disease surfaces; +H = baseline + HMIS test-positivity rate; +Hc = baseline + HMIS-calibrated prevalence; +Ap = baseline + archetype P. falciparum prevalence; +Af = baseline + full archetype set; +HA = baseline + HMIS + full archetype set; +M = baseline + MAP intervention rasters. Every set augments the ten-covariate baseline; none removes a baseline covariate. Set sizes range from 10 (baseline) to 14 (+HA) covariates. ✓indicates inclusion.

2.7 Sensitivity and Structural-robustness Analyses

Three further analyses tested whether the primary model's structural choices materially affected its conclusions. First, the discrete queen-contiguity BYM2 spatial field was compared against a continuous Gaussian Matérn random field (stochastic partial differential equation, SPDE, approximation [23], [24]), fitted directly on the geographic coordinates of the 561 usable 2021 NMIS clusters and predicted to LGA centroids. This comparison used cluster-level data. Only five covariates were available at that resolution: MAP parasite rate, enhanced vegetation index, aridity, elevation, and population density. A further variant added the ITN use, IRS coverage, and P. falciparum mortality rasters. Five covariates used in the primary model (household wealth, health-facility density, proportion urban, precipitation, and maximum temperature) are defined only at LGA level and were therefore excluded. Because the covariate sets differ, WAIC values from this comparison are interpretable only within the SPDE analysis itself. Variants adding an LGA-level unstructured (iid) term alongside the continuous field, and variants allowing a separate, shorter-range urban-specific field alongside a national-scale field, were also fitted. Second, RDT and microscopy were fitted jointly, sharing a single BYM2 spatial field scaled by an estimated diagnostic-specific factor (delta; shared-component joint disease mapping, following Held et al. [25]), with an additional state-level random intercept on microscopy's linear predictor to permit the RDT-microscopy relationship to vary regionally. Third, the primary LGA-only BYM2 model was compared against models adding a state-level or NMEP geopolitical zone-level unstructured random effect on top of the existing LGA-level spatial field. Calibration of all three alternatives was assessed with probability integral transform (PIT) histograms, on the same basis as the primary model.

3. Results

The 2021 NMIS provided direct observational data for 422 (54.5%) of Nigeria’s 774 LGAs, with each containing at least one sampled cluster; the remaining 352 (45.5%) contained none and could only be described through spatial smoothing and covariate information (Figure 1). Uncovered LGAs were not distributed uniformly, with contiguous gaps most evident across parts of the north-central and north-eastern zones. Among the 422 data-informed LGAs, direct cluster-based prevalence estimates, calculated from the sampled clusters alone with no modelling, ranged from 0% to 100% for both diagnostics (mean 35.4% RDT, 20.0% microscopy), a spread that could be driven substantially by small within-LGA sample sizes rather than by true prevalence swings of that magnitude. Both the coverage gap and this direct-estimate noise motivate a model-based approach capable of borrowing strength across space and covariates, whose specification is evaluated next.

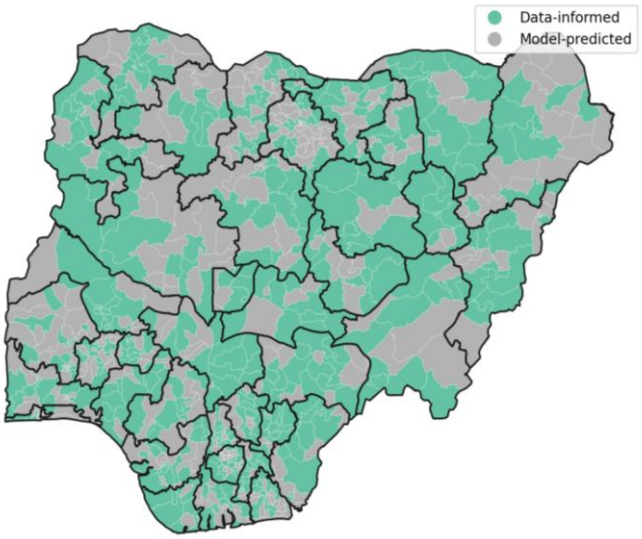


Figure 1. LGA-level survey coverage, 2021 NMIS. Data-informed LGAs contained at least one survey cluster; model-predicted LGAs contained none. State boundaries are shown in black; LGA boundaries in white.1

In terms of model comparison and calibration, across the eight candidate covariate sets (Table 1), the baseline set augmented with the global P. falciparum prevalence and incidence surfaces gave the lowest WAIC and DIC for both diagnostics (Table 2). For RDT this set was clearly preferred (ΔDIC = 12.1, ΔWAIC = 9.3 against the next-best set). For microscopy the candidate sets were closely matched (ΔDIC = 2.9, ΔWAIC = 1.9) and were not distinguishable on these criteria; the same set was therefore retained for microscopy to maintain a common covariate specification across the two diagnostics.

Table 2. Covariate-set comparison (best four of eight candidates per diagnostic)2

Outcome	Covariate set	n covariates	DIC	WAIC
Microscopy	Baseline + global †	12	1681.0	1672.7
Microscopy	Baseline + HMIS	11	1683.9	1674.6
Microscopy	Baseline	10	1684.4	1675.5
Microscopy	Baseline + MAP layers	13	1685.3	1675.7
RDT	Baseline + global †	12	1890.5	1877.7
RDT	Baseline + MAP layers	13	1902.6	1887.0
RDT	Baseline + HMIS	11	1902.9	1887.9
RDT	Baseline	10	1903.0	1888.2

† Lowest WAIC

Posterior fixed effect estimates for the final model are reported in Table 3. Three covariates had a 95% credible interval excluding zero for at least one diagnostic. Higher household wealth

was associated with lower prevalence, and higher values of the global P. falciparum prevalence surface were associated with higher local prevalence, for both RDT and microscopy. Higher enhanced vegetation index was associated with higher prevalence for RDT, but its credible interval included zero for microscopy.

Table 3. Posterior fixed-effect estimates for the final model (log-odds scale)3

Covariate	RDT, mean (95% CrI)	Microscopy, mean (95% CrI)
Intercept	-0.73 (-0.82, -0.64)	-1.70 (-1.80, -1.60)
Enhanced vegetation index	0.22 (0.02, 0.42)*	0.23 (-0.01, 0.47)
Aridity index	0.06 (-0.33, 0.45)	0.03 (-0.57, 0.63)
Elevation	0.09 (-0.10, 0.29)	-0.04 (-0.28, 0.20)
Household wealth index	-0.62 (-0.77, -0.47)*	-0.80 (-0.98, -0.62)*
Health-facility density (per 1,000 under-five)	0.04 (-0.08, 0.15)	0.02 (-0.12, 0.15)
Population density	0.03 (-0.14, 0.20)	0.10 (-0.10, 0.29)
Proportion urban	0.02 (-0.09, 0.13)	0.00 (-0.13, 0.13)
Precipitation, 2021	0.06 (-0.29, 0.42)	-0.12 (-0.60, 0.37)
Maximum temperature, 2021	0.11 (-0.16, 0.38)	-0.17 (-0.51, 0.17)
MAP P. falciparum prevalence, global product	0.66 (0.31, 1.01)*	0.51 (0.08, 0.94)*
MAP P. falciparum incidence, global product	0.06 (-0.37, 0.49)	-0.12 (-0.66, 0.42)

** 95% credible interval excludes zero. Covariates were standardised (zero mean, unit variance) prior to fitting, so coefficients are comparable in scale within each diagnostic but not across diagnostics.*

The prevalence estimates show that both diagnostics reproduced the established northwest-to-southeast prevalence gradient (Figure 2), with the highest estimates in Kebbi, Zamfara, Katsina, and Sokoto States and the lowest in Lagos State (Table 4). Population-weighted zonal means were highest in the Northwest (47.2% RDT, 25.5% microscopy) and Northeast (36.8% RDT, 15.5% microscopy), intermediate in North Central (29.0% RDT, 15.4% microscopy), and lowest and broadly similar across the three southern zones (24.8–29.7% RDT, 14.9–17.4% microscopy). Uncertainty followed the survey coverage gap: mean 95% credible interval (CrI) width was narrower in data-informed than in model-predicted LGAs for both diagnostics, 29.5 versus 53.4 percentage points for RDT and 24.0 versus 42.8 percentage points for microscopy, while mean prevalence was similar between the two groups, indicating that the coverage gap affected precision rather than the central estimate.

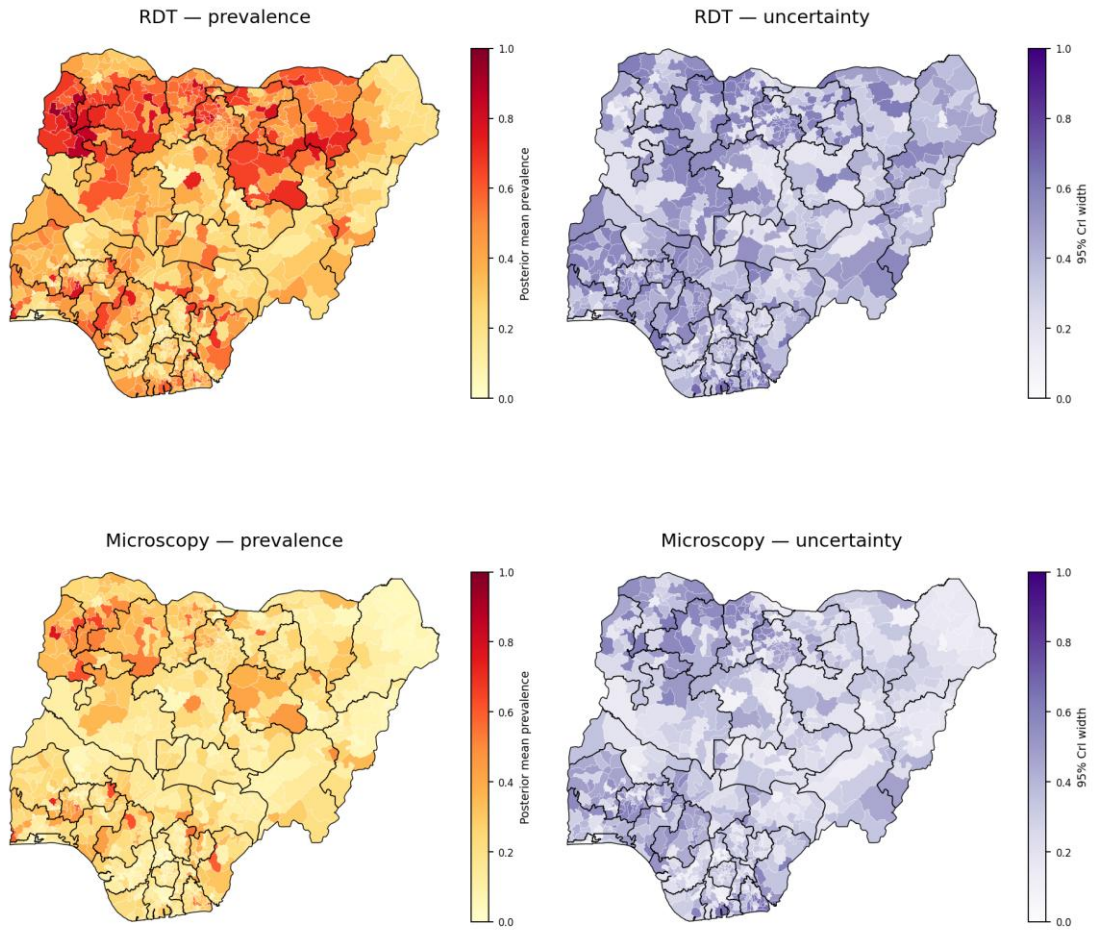


Figure 2. LGA-level posterior mean prevalence (left) and 95% credible interval width (right), by diagnostic. State boundaries shown in black; LGA boundaries in white.2

Table 4. Highest- and lowest-prevalence LGAs, ranked by microscopy4

LGA	State	Microscopy (95% CrI)	RDT (95% CrI)
Highest microscopy prevalence			
Bunza	Kebbi	76.3 (67.5–83.7)	93.3 (87.9–96.8)
Udung Uko	Akwa Ibom	75.4 (56.8–88.8)	69.4 (51.0–84.1)
Akinyele	Oyo	72.2 (54.8–85.7)	72.4 (55.5–85.6)
Aleiro	Kebbi	68.7 (51.4–82.8)	82.3 (67.7–92.1)
Lowest microscopy prevalence			
Amuwo Odofin	Lagos	1.0 (0.2–3.2)	1.4 (0.3–4.1)
Lagos Mainland	Lagos	1.3 (0.2–4.3)	1.6 (0.3–4.9)
Gombe	Gombe	1.8 (0.4–5.4)	11.4 (5.1–21.3)

For both diagnostics, model-predicted LGAs are shifted toward markedly wider intervals than data-informed LGAs, but the two distributions are only partially separated rather than cleanly split: some data-informed LGAs, typically those with small cluster samples, have intervals as wide as the model-predicted median, and some model-predicted LGAs, typically those with strong covariate or neighbouring-LGA support, achieve intervals as narrow as the data-informed median (Figure 3).

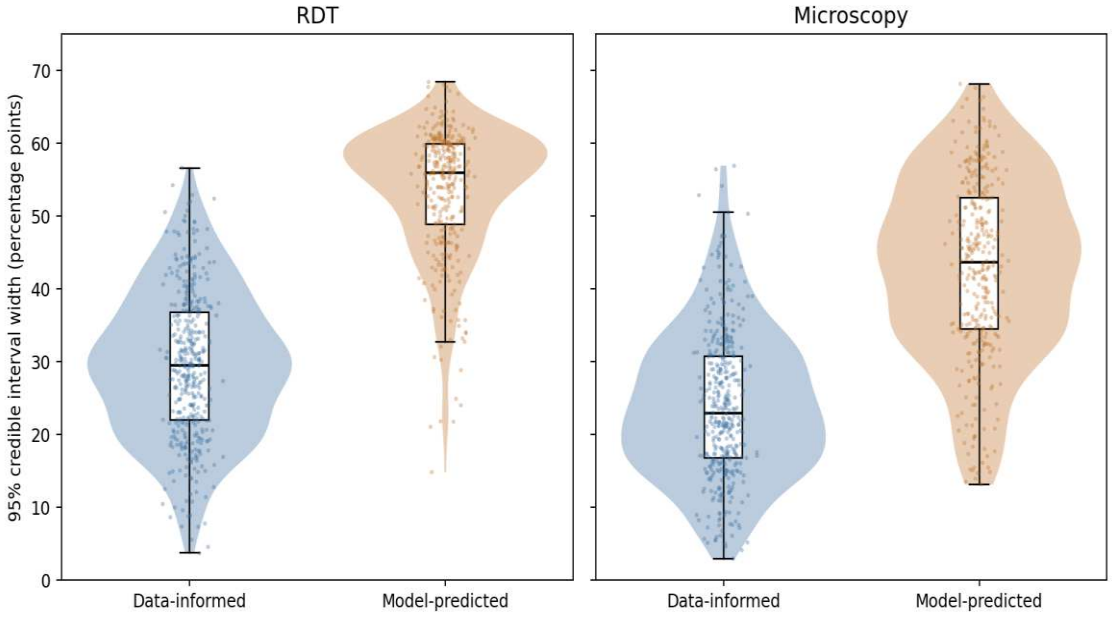


Figure 3. Distribution of 95% credible interval width by data source and diagnostic. Violin shapes show the full distribution across LGAs; boxes show the median and interquartile range; points are individual LGAs. The two distributions overlap, some data-informed LGAs still have wide intervals (typically those with small cluster samples) and some model-predicted LGAs have comparatively narrow ones (typically those with strong covariate or neighbouring-LGA information), but model-predicted LGAs are shifted markedly wider overall.3

Applying the National Malaria Strategic Plan's (NMSP) five operational prevalence cutoffs to the primary model's posterior means classifies 48.6% of LGAs as High and 40.7% as Moderate A by RDT, against only 10.6% High and 49.9% Moderate A by microscopy. A striking diagnostic-dependent difference specifically in how many LGAs land in the country's highest-priority transmission tier: RDT classifies close to half the country as High, while microscopy classifies barely one in ten LGAs the same way. This gap is directly attributable to RDT's higher sensitivity and lower specificity relative to microscopy rather than to any difference in how the two models were fitted, and is visually obvious in Figure 4, where the RDT map is dominated by the darkest (High) shading across most of the northern half of the country while the microscopy map for the same LGAs is predominantly the lighter Moderate A and Moderate B shades. No LGA fell into the Very Low (<1%) band under either diagnostic, and Low B and Low A together account for only 5.5% of LGAs by RDT against 18.8% by microscopy (Figure 5).

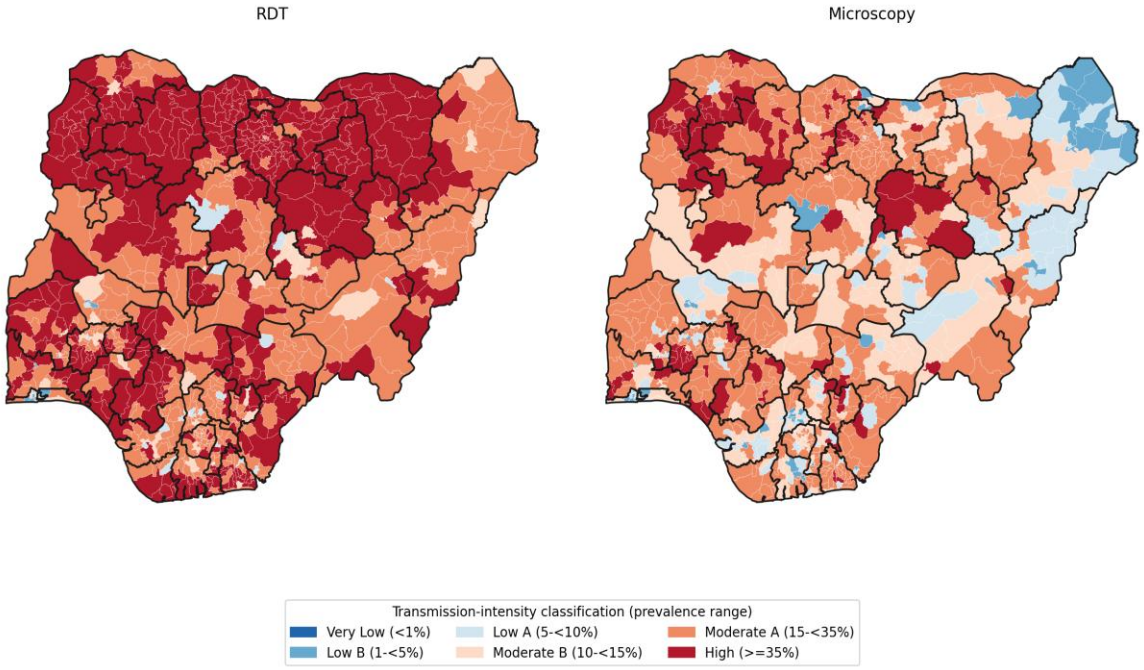


Figure 4. Transmission-intensity classification, by diagnostic. Category definitions (prevalence ranges) are shown in the legend. State boundaries shown in black; LGA boundaries in white4

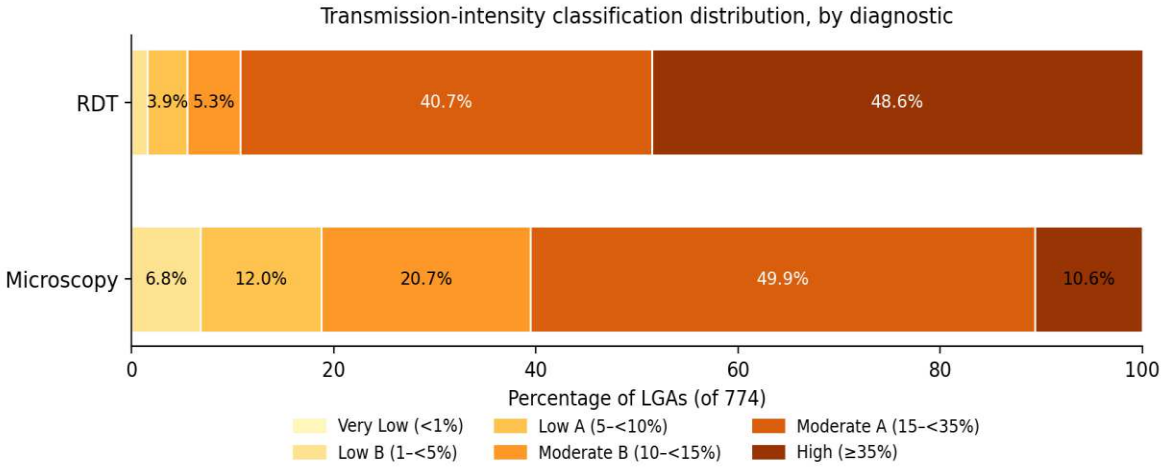


Figure 5. Transmission-intensity classification distribution (% of 774 LGAs), by diagnostic5

Table 5 summarises the three structural-robustness checks. The continuous-space and hierarchical-pooling alternatives corroborate the primary model's structure without changing its conclusions; the joint diagnostic model adds a new finding. Fitting the two diagnostics together gave a lower combined WAIC (3381.7) than the sum of the two independent models (3550.4), and the estimated scaling factor of 1.09 (95% CrI 0.96-1.22) indicates that RDT and microscopy share a common national-scale spatial pattern of essentially the same amplitude. Their local disagreement, however, is not uniform: the state-level microscopy offset was credibly non-zero in 9 of 37 states (Table 6), showing that RDT-microscopy discordance is regionally structured rather than a constant national offset.

Table 5. Summary of structural-robustness analyses. Full model-comparison tables and calibration figures for all three structural-robustness analyses are in Additional file 1 (see individual cells for specific table/figure numbers).5

Alternative specification tested	Key result	Implication for the primary model
Continuous-space (SPDE) spatial field vs. discrete BYM2 adjacency (cluster-level, reduced covariate set)	Covariate-set WAIC ordering matched the primary model; adding an LGA-level unstructured term further improved fit (Supp. Table S1-S2). Calibration was notably poorer than the primary model's own PIT check (Supp. Figure S2).	Supports the primary model's combination of structured + unstructured spatial variance. Does not provide reliable independent evidence on individual covariates (e.g., aridity), given its own calibration weakness.
State- or zone-level pooling added on top of the primary LGA-level BYM2 field	WAIC improved by at most 2.8 points; added group-level variance was shrunk to near zero (Supp. Table S3).	The LGA-level spatial field already captures the poolable structure; coarser grouping adds no meaningful value.
Joint RDT+microscopy model with a shared, diagnostic-scaled spatial field, vs. independent models	Combined WAIC (3381.7) below the sum of the independent models' WAICs (3550.4). National scaling factor delta = 1.09 (95% CrI 0.96-1.22). A state-level microscopy offset had a credible interval excluding zero in 9 of 37 states (Table 6).	RDT and microscopy share a common national-scale spatial pattern, but the size of their local disagreement varies meaningfully by state, a direct refinement of the transmission-tier discordance reported.

Table 6 lists the six states with the largest-magnitude, credibly non-zero microscopy-specific offset from the joint model (the full 37-state list and underlying model specification are in Additional file 1: Table S4).

Table 6. States with the largest credibly non-zero microscopy-specific offset in the joint model. Full 37-state list in Additional file 1: Table S46

State	Offset, mean (log-odds)	95% CrI
Yobe	-0.78	-1.11 to -0.46
Sokoto	+0.65	0.34 to 0.96
Ebonyi	+0.53	0.19 to 0.87
Akwa Ibom	+0.49	0.12 to 0.85
Rivers	-0.47	-0.90 to -0.04
Jigawa	-0.40	-0.70 to -0.10

These results show that RDT and microscopy classify LGAs very differently nationally, and the joint model shows this reflects a shared national spatial pattern combined with real, state-specific local divergence, not a single uniform bias. Practically, this suggests NMEP guidance on diagnostic choice for resource allocation may need to be state-sensitive in at least the states listed in Table 6, rather than a single nationwide rule.

4. Discussion

This study extends Bayesian small area estimation (SAE) of malaria prevalence to Nigeria's full complement of 774 LGAs using the 2021 NMIS, building on ward-level work in Ghana [8] and subnational work in Zambia [26]. As in those studies, spatial smoothing under BYM2

allowed prevalence to be estimated in the 352 LGAs (45.5%) with no surveyed cluster, at the cost of wider credible intervals relative to the 422 LGAs with direct data.

These findings connect directly to the 2021 NMIS's own direct, design-based zonal estimates. Population-weighted estimates here are consistently lower than the survey's direct estimates in the three northern zones: North West (47.2% RDT, 25.5% microscopy here vs. 51.6%/29.8% direct), North East (36.8%/15.5% vs. 43.0%/20.1%), and North Central (29.0%/15.4% vs. 32.3%/17.0%). The three southern zones agree far more closely (24.8-29.7% RDT / 14.9-17.4% microscopy here, spanning the direct South East, South South, and South West estimates of 27.3%/18.7%, 29.9%/17.8%, and 24.1%/16.2%). Because northern survey coverage is thinnest, this is consistent with spatial smoothing pulling data-sparse northern LGAs toward lower, covariate- and neighbour-supported values, understating burden where it is both highest and least directly measured.

The posterior estimates show Bunza and Aleiro LGAs in Kebbi State consistently among the highest-prevalence areas (Table 4), reinforcing north-western Nigeria's status as a major transmission hotspot [27]. Udung Uko in Akwa Ibom and Akinyele in Oyo also emerged among the highest-prevalence LGAs despite their southern location, showing that hotspots can persist outside traditionally recognised high-burden regions. Conversely, Amuwo Odofin and Lagos Mainland in Lagos State recorded the lowest estimates, consistent with reduced transmission in highly urbanised settings with better housing, sanitation, and healthcare access. Gombe LGA's low prevalence, despite its northern location, illustrates the epidemiological heterogeneity that persists even within high-transmission regions.

The overlap in credible interval widths between data-informed and model-predicted LGAs indicates that precision depends on overall evidential strength rather than survey coverage alone. Some unsampled LGAs achieved precision comparable to sampled areas through strong neighbouring or covariate support, while some data-informed LGAs remained uncertain. This demonstrates a key advantage of Bayesian SAE: information can be borrowed adaptively across areas and covariates rather than relying solely on direct observations [28]. Similar findings have been reported in other Bayesian disease-mapping studies combining survey and routine data to improve estimation in data-sparse areas [29].

The marked differences in transmission-intensity classification between RDT and microscopy have important implications for stratification and programme implementation. Both diagnostics identified broadly similar geographical patterns, but nearly half of LGAs were classified as High transmission by RDT compared with about one in ten by microscopy. This difference is consistent with Nigeria's survey history, where RDT-microscopy prevalence gaps increased from about 10 percentage points in 2010 to 18 points in 2015 [30], and reflects differences in diagnostic properties. HRP2-based RDTs can remain positive after parasite clearance because they detect persistent antigens, whereas microscopy directly detects circulating parasites and is more conservative, though less sensitive at low parasite densities [31]. In the 2021 NMIS, RDT sensitivity was 88.6% and specificity 75.2% against microscopy [32], helping explain the greater number of LGAs classified as High transmission using RDT. Thus, the larger RDT-based count reflects the broader infection history captured by antigen detection rather than overestimation by the Bayesian model.

The model combining baseline covariates with global *P. falciparum* prevalence and incidence surfaces outperformed other candidate specifications, with a stronger improvement for RDT than microscopy. Its selection for both diagnostics suggests that global malaria products capture spatial variation not fully explained by local environmental and health-system covariates, supporting the use of external geospatial information in Bayesian SAE where survey coverage is sparse. Similar improvements from auxiliary spatial covariates have been reported in Angola [33], Côte d'Ivoire [34], Rwanda [29], and Ghana [8].

Fixed-effect estimates indicated that socioeconomic conditions and underlying transmission intensity were the strongest determinants of prevalence after accounting for spatial dependence. Household wealth was inversely associated with prevalence across both diagnostics, consistent with the established relationship between socioeconomic deprivation and malaria risk [35]. The positive association between the global *P. falciparum* prevalence surface and local estimates further supports the integration of established risk surfaces into SAE models where local covariates alone are insufficient.

Most environmental covariates, including precipitation, temperature, elevation, aridity, population density, and urbanicity, did not have credible intervals excluding zero after adjustment for spatial random effects. This likely reflects spatial confounding, whereby structured random effects absorb residual spatial dependence, making it difficult to distinguish the effects of spatially structured covariates from the spatial term [36]. The positive RDT association with enhanced vegetation index is biologically plausible, but its absence in the microscopy model suggests caution in interpreting it as a distinct ecological mechanism.

The 352 LGAs (45.5%) without surveyed clusters represent not only a modelling limitation but also a resource-mobilisation signal. They identify areas where future MIS or DHS rounds could gain most from oversampling and where routine HMIS data quality is particularly important for interim triangulation. We therefore recommend prioritising these LGAs, particularly contiguous gaps in the north-central and north-eastern zones, for additional cluster allocation in the next survey round.

The NMSP 2021–2025 already assigns differentiated intervention mixes by stratum, including SMC for high-seasonality Sahel/Savannah states, IRS as an acceleration or push-to-elimination tool, and ITN microstratification in large urban areas [37]. Kebbi, Zamfara, and Sokoto, identified here as highest-burden areas, are already on the plan's IRS-targeting list. The LGA-level estimates can support more precise targeting of IRS or SMC to high-tier LGAs rather than applying interventions uniformly across states.

Diagnostic choice is therefore not merely a methodological detail but a determinant of resource-allocation outcomes. NMEP originally commissioned this analysis for microscopy-based LGA-level estimates to support the 2026–2030 National Malaria Strategic Plan, but the scope was expanded to include RDT because successive MIS rounds showed widening prevalence differences between the diagnostics. Across most of Nigeria, the two diagnostics followed a shared spatial pattern; however, in Yobe, Sokoto, Ebonyi, Akwa Ibom, Rivers, and Jigawa, their relationship diverged credibly, meaning that reliance on RDT alone could produce materially different allocation decisions from microscopy. Rather than nationwide confirmatory testing, targeted confirmatory microscopy or PCR in these six states may be more efficient.

These findings carry implications beyond programme efficiency. Sustainable Development Goal 3 commits to ensuring healthy lives at all ages, with target 3.3 specifically calling for an end to the malaria epidemic and target 3.8 for universal health coverage including access to effective essential health services [38]. Achieving these targets in Nigeria, which bears the world's largest malaria burden, depends on allocating limited resources to the districts where they are most needed, using evidence that is both granular and reliable. The LGA-level estimates produced here provide that evidence base at the resolution NMEP's planning cycle requires. Equally, the finding that unexamined diagnostic choice can silently redirect resources away from or toward specific states exposes an equity dimension that aggregate national statistics cannot reveal. Addressing this gap, by designating a diagnostic standard for classification or by adjusting thresholds to account for diagnostic properties, is a prerequisite for ensuring that stratified intervention planning serves the populations at greatest risk rather than reflecting measurement artefacts. In this sense, the contribution is not only technical but structural: it strengthens the evidence infrastructure on which equitable progress toward SDG 3 depends.

5. Limitations of the Study

These findings should be interpreted in light of several limitations. First, the absence of 2021 NMIS clusters in 352 LGAs means that estimates for almost half of the country depend on spatial contiguity and the selected covariates adequately capturing prevalence drivers in unsampled areas. The BYM2 spatial term may smooth genuine local departures caused by factors such as localised vector-control campaigns or population displacement due to conflict.

Second, the cross-sectional 2021 NMIS provides a snapshot of malaria transmission during the survey period. Given malaria's seasonality, the estimates may not reflect subsequent changes associated with interventions, treatment policies, or emerging pyrethroid resistance.

Third, neither RDT nor microscopy is a gold standard; both are imperfect measures of infection and have known, partly compensating error profiles. Each study model is studied individually and does not compare with a PCR confirmed diagnosis, which was not available in the NMIS. The range of divergence found in the diagnostic test discussion, therefore, is not the range of the “true” prevalence of infection in the biological realm, but rather the range between the estimates produced by the various instruments. Such a validation exercise would need to include molecular diagnostics in a representative subsample to determine which estimate is closer to the true prevalence of infection in the biological realm.

Fourth, the covariates vary in vintage, spatial resolution, and provenance. Although standardisation placed them on a common modelling scale, it did not eliminate their underlying measurement error. Calibration of routine-system data introduces additional uncertainty that is not fully propagated in the reported credible intervals.

Fifth, prevalence data were restricted to children aged 6–59 months, the standard MIS age range. Although this population experiences substantial malaria burden and is central to many control interventions, the estimates cannot be assumed to represent older children or adults. Finally, transmission-intensity classification used the NMSP's current five-tier thresholds without adjustment for diagnostic differences.

6. Conclusions

This study created national, LGA-level, Bayesian small-area estimates of malaria prevalence for Nigeria, with direct survey observation in 422 LGAs and covariate- and neighbour-informed prediction in the remaining 352. The resulting maps reproduce the established transmission gradient from the north-west to south-east of Nigeria at a resolution that will allow NMEP to choose LGAs on which to base programme planning, and to have a principled basis for deciding which LGAs are well-characterised and which are not and would benefit from further ground-truthing.

The most important of these findings is not the pattern itself but the sensitivity of the pattern to the diagnostic. This difference in the classification between RDT and microscopy is significant: under NMSP's current tier system, about half of all LGAs would be classified in the High tier by the RDT and only about 10% by the microscopy classification, indicating that choice of measurement is not a minor technical detail, but rather a factor that would shape the national distribution of intervention resources. This has a clear implication for practice: in an increasingly RDT dominated reporting environment, NMEP should consider the need to explicitly designate a single diagnostic event for the basis of tier-based resource allocation decisions, or to reassess the appropriateness of the existing five-tiers. In addition to the estimates, the interactive dashboard associated with the study aims to bridge the gap between the rigorous Bayesian application and practical use by non-statisticians amongst programme staff, continuing the recent trend of marrying S.A.E. with easy-to-use visual tools [7, 9].

There is also value in extending this analytical approach downward to the ward level to strengthen the granularity of intervention targeting further. As future MIS rounds become available, successive application of this framework would enable trend monitoring at LGA level, supporting adaptive programme planning in Nigeria and offering a transferable model for comparable settings across sub-Saharan Africa.

Abbreviations

Abbreviation	Full Meaning
BYM	Besag–York–Mollié Model
BYM2	Reparameterised Besag–York–Mollié Model
CPO	Conditional Predictive Ordinate
CrI	Credible Interval
DHS	Demographic and Health Survey
DIC	Deviance Information Criterion
GPS	Global Positioning System

GRID3	Geo-Referenced Infrastructure and Demographic Data for Development
HMIS	Health Management Information System
ICAR	Intrinsic Conditional Autoregressive Model
INLA	Integrated Nested Laplace Approximation
IRS	Indoor Residual Spraying
ITN	Insecticide-Treated Net
LGA	Local Government Area
LGAs	Local Government Areas
LMICs	Low- and Middle-Income Countries
MAP	Malaria Atlas Project
MIS	Malaria Indicator Survey
NMEP	National Malaria Elimination Programme
NMIS	Nigeria Malaria Indicator Survey
PC	Penalised Complexity (Prior)
PIT	Probability Integral Transform
RDT	Rapid Diagnostic Test
SAE	Small Area Estimation
WAIC	Watanabe–Akaike Information Criterion
DHIS2	District Health Information System 2
HRP2	Histidine-Rich Protein 2
NMSP	National Malaria Strategic Plan
SPDE	Stochastic Partial Differential Equation

Declarations

Ethics approval and consent to participate

Not applicable.

Consent for publication

Not applicable.

Availability of data and materials

The 2021 Nigeria Malaria Indicator Survey (NMIS) microdata used in this analysis are available on registered application to the DHS Program (www.dhsprogram.com). LGA boundary files were obtained from GRID3 Nigeria. Malaria Atlas Project (MAP) surfaces are publicly available via the malariaAtlas R package; WorldClim and WorldPop covariates are publicly available from their respective repositories. The routine HMIS test-positivity data was obtained from District Health Information System 2 (DHIS2) and granted access by the National Malaria Elimination Programme (NMEP), Nigeria. Requests for access should be directed to NMEP.

Competing interests

The authors declare that they have no competing interests.

Funding

No specific funding was received for this work.

Authors' contributions

OA designed the study, performed the statistical and spatial modelling analyses, and wrote the first draft of the manuscript. MR conducted the literature review and contributed to drafting and revising the manuscript, and to data cleaning and triangulation. DB contributed to data cleaning and triangulation and to drafting and revising the manuscript. AC contributed to data collection, cleaning and triangulation, and to drafting and revising the manuscript. DO contributed to the literature review and served as the study's liaison with the NMEP. OC and AE reviewed the manuscript. EN, GN, NO and CO reviewed the manuscript to ensure its findings and recommendations align with national malaria control programmatic priorities. EG critically reviewed the manuscript's statistical and spatial methodology. GE critically reviewed the manuscript and ensured alignment with national malaria control policy and strategy. CK is the Principal Investigator, conceived the study, provided overall supervision, and critically reviewed the manuscript. All authors read and approved the final manuscript.

Acknowledgements

The authors thank the DHS Program for access to the 2021 NMIS microdata and Nigeria's National Malaria Elimination Programme for programmatic context and access to routine HMIS data.

References

1. Mahama T. Bayesian hierarchical modeling for small-area estimation of disease burden. Int J Sci Res Arch. 2022;7(2):807-27.

2. Abubakar EO, Cunningham N. Small-area estimation and analysis of HIV/AIDS indicators for precise geographical targeting of health interventions in Nigeria: a spatial microsimulation approach. Int J Health Geogr. 2023;22:23.

3. World Health Organization. Report on malaria in Nigeria 2022. Brazzaville: WHO Regional Office for Africa; 2023.

4. Adigun AB, Gajere EN, Oresanya O, Vounatsou P. Malaria risk in Nigeria: Bayesian geostatistical modelling of 2010 malaria indicator survey data. Malar J. 2015;14:156.

5. Omojuyigbe JO, Owolade AJ-J, Sokunbi TO, Bakenne HA, Ogungbe BA, Oladipo HJ, et al. Malaria eradication in Nigeria: state of the nation and priorities for action. J Med Surg Public Health. 2023;1:100024.

6. Ozodiegwu ID, Ambrose M, Galatas B, Runge M, Nandi A, Okuneye K, et al. Application of mathematical modelling to inform national malaria intervention planning in Nigeria. Malar J. 2023;22:137.

7. Sironi A, Bertoldo J, Sampaio V, Coimbra D, Rasella D, Barreto ME. Malaria-VisAnalytics: a tool for visual exploratory analysis of Brazilian public malaria data. Malar J. 2022;21:232.

8. Aheto JMK. Mapping under-five child malaria risk that accounts for environmental and climatic factors to aid malaria preventive and control efforts in Ghana: Bayesian geospatial and interactive web-based mapping methods. Malar J. 2022;21:384.

9. Wu Y, Dong Q, Xu J, Li ZR, Wakefield J. sae4health: an R Shiny application for small area estimation in low- and middle-income countries. arXiv. 2025. https://arxiv.org/pdf/2505.01467

10. Wakefield J, Okonek T, Pedersen J. Small area estimation for disease prevalence mapping. Int Stat Rev. 2020;88(2):398-418.

11. Oso TA, Okesanya OJ, Adebayo UO, Ayelaagbe OB, Ahmed MM, Obadeyi KB, et al. Spatial and temporal inequalities in malaria incidence and mortality among children aged 0-4 years in Nigeria: a subnational analysis, 2010-2019. Malar J. 2026;25:126.

12. Bayode T, Siegmund A. Identifying childhood malaria hotspots and risk factors in a Nigerian city using geostatistical modelling approach. Sci Rep. 2024;14:1-13.

13. Besag J, York J, Mollié A. Bayesian image restoration, with two applications in spatial statistics. Ann Inst Stat Math. 1991;43(1):1-20.

14. Cameron E, Battle KE, Bhatt S, Weiss DJ, Bisanzio D, Mappin B, et al. Defining the relationship between infection prevalence and clinical incidence of Plasmodium falciparum malaria. Nat Commun. 2015;6:8170.

15. Riebler A, Sørbye SH, Simpson D, Rue H. An intuitive Bayesian spatial model for disease mapping that accounts for scaling. Stat Methods Med Res. 2016;25(4):1145-65.

16. Sørbye SH, Rue H. Scaling intrinsic Gaussian Markov random field priors in spatial modelling. Spat Stat. 2014;8:39-51.

17. Simpson D, Rue H, Riebler A, Martins TG, Sørbye SH. Penalising model component complexity: a principled, practical approach to constructing priors. Stat Sci. 2017;32(1):1-28.

18. Rue H, Martino S, Chopin N. Approximate Bayesian inference for latent Gaussian models by using integrated nested Laplace approximations. J R Stat Soc Series B Stat Methodol. 2009;71(2):319-92.

19. National Malaria Elimination Programme. *National malaria strategic plan 2026–2030*. Abuja: National Malaria Elimination Programme; 2026.

20. World Health Organization. *Malaria surveillance, monitoring and evaluation: a reference manual*. 2nd ed. Geneva: World Health Organization; 2025.

21. Watanabe S. Asymptotic equivalence of Bayes cross validation and widely applicable information criterion in singular learning theory. J Mach Learn Res. 2010;11:3571-94.
22. Spiegelhalter DJ, Best NG, Carlin BP, van der Linde A. Bayesian measures of model complexity and fit. J R Stat Soc Series B Stat Methodol. 2002;64(4):583-639.
23. Held L, Schrödle B, Rue H. Posterior and cross-validatory predictive checks: a comparison of MCMC and INLA. In: Kneib T, Tutz G, editors. Statistical Modelling and Regression Structures. Heidelberg: Physica-Verlag; 2010. p. 91-110.
24. Lindgren F, Rue H, Lindström J. An explicit link between Gaussian fields and Gaussian Markov random fields: the stochastic partial differential equation approach. J R Stat Soc Series B Stat Methodol. 2011;73(4):423-98.
25. Held L, Natário I, Fenton SE, Rue H, Becker N. Towards joint disease mapping. Stat Methods Med Res. 2005;14(1):61-82.
26. Kalindi AM, Das S. Disaggregated level child morbidity in Zambia: an application of small area estimation method. Popul Health Metr. 2025;23:51.
27. National Malaria Elimination Programme (NMEP), National Population Commission (NPC), ICF. Nigeria Malaria Indicator Survey 2021 Final Report. Abuja, Nigeria, and Rockville, Maryland, USA: NMEP, NPC, and ICF; 2022.
28. Rao JNK, Molina I. Small Area Estimation. 2nd ed. Hoboken: Wiley; 2015.
29. Semakula M, Niragire F, Faes C. Spatio-temporal Bayesian models for malaria risk using survey and health facility routine data in Rwanda. Int J Environ Res Public Health. 2023;20(5):4283.
30. Fagbamigbe AF. On the discriminatory and predictive accuracy of the RDT against the microscopy in the diagnosis of malaria among under-five children in Nigeria. Malar J. 2019;18:46.
31. Kyabayinze DJ, Tibenderana JK, Odong GW, Rwakimari JB, Counihan H. Operational accuracy and comparative persistent antigenicity of HRP2 rapid diagnostic tests for Plasmodium falciparum malaria in a hyperendemic region of Uganda. Malar J. 2008;7:221.
32. Olubiyi B, Alabi A, Isiko I. Field performance of the SD Bioline Malaria Ag P.f. rapid diagnostic test among children under five in Nigeria: insights from the 2021 Malaria Indicator Survey. Malar J. 2026;25:115.
33. Gosoniu L, Veta AM, Vounatsou P. Bayesian geostatistical modeling of Malaria Indicator Survey data in Angola. PLoS ONE. 2010;5(3):e9322.
34. Raso G, Schur N, Utzinger J, Koudou BG, Tchicaya ES, Rohner F, et al. Mapping malaria risk among children in Côte d'Ivoire using Bayesian geo-statistical models. Malar J. 2012;11:160.

35. Degarege A, Fennie K, Degarege D, Chennupati S, Madhivanan P. Improving socioeconomic status may reduce the burden of malaria in sub-Saharan Africa: a systematic review and meta-analysis. PLoS ONE. 2019;14(1):e0211205.
36. Azevedo DRM, Bandyopadhyay D, Prates MO, Abdel-Salam AG, Garcia D. Assessing spatial confounding in cancer disease mapping using R. Cancer Rep. 2020;3(4):e1263.
37. Federal Ministry of Health. National Malaria Strategic Plan 2021-2025. Abuja: Federal Ministry of Health, Nigeria; 2021.
38. United Nations, Department of Economic and Social Affairs Sustainable Development. Ensure healthy lives and promote well-being for all at all ages.